

RIJKSUNIVERSITEIT GRONINGEN

---

# Light shift in a single $\text{Ba}^+$ ion

---

BACHELOR THESIS

*Author:*  
Aswin Hofsteenge

*Supervisors:*  
Prof. Dr. K.H.K.J Jungmann  
Dr. L. Willmann

July 2015

# Contents

<b>1</b>	<b>Introduction</b>	<b>1</b>
1.1	Atomic Parity Violation . . . . .	3
1.2	Light shift to measure Atomic Parity Violation . . . . .	6
<b>2</b>	<b>Experimental Setup</b>	<b>7</b>
2.1	Concept of the experiment . . . . .	7
2.2	How to trap a single ion . . . . .	9
2.2.1	Ion trap . . . . .	9
2.2.2	Ion source . . . . .	9
2.2.3	Testing the oven in a vacuum chamber . . . . .	10
2.2.4	Testing the oven with a laser . . . . .	11
2.2.5	Creating one single ion . . . . .	13
2.3	Vacuum Chamber . . . . .	13
2.4	Lasers . . . . .	14
2.4.1	Ion cooling with lasers . . . . .	15
2.4.2	Second harmonic generation . . . . .	16
2.4.3	Frequency comb . . . . .	18
2.4.4	The barium test laser . . . . .	20
2.4.5	Light shift laser . . . . .	21
2.4.6	The cooling and detection lasers . . . . .	21
2.4.7	Photoionization laser . . . . .	22
2.5	Data acquisition . . . . .	23
<b>3</b>	<b>Measurement plan for the experiment</b>	<b>24</b>
3.1	Different parameters . . . . .	25
3.1.1	Laser power . . . . .	26
3.1.2	Laser detuning . . . . .	27
3.1.3	Field gradients . . . . .	28
3.1.4	Magnetic fields . . . . .	28
3.1.5	Polarization . . . . .	29
3.2	Measuring a light shift . . . . .	30
<b>4</b>	<b>Conclusion</b>	<b>32</b>
4.1	Conclusion . . . . .	32

**Bibliografy**

**33**

**Acknowledgements**

**35**

# Chapter 1

## Introduction

In this experiment the light shift of singly charged barium ions ( $\text{Ba}^+$ ) is investigated. If an atomic system is placed in an intense light field, its energy levels experience light shifts. Light shift means that the energy levels of an atomic system are shifted with respect to each other. By measuring the light shift of well known atomic systems such as, e.g.  $\text{Ba}^+$  ions or singly charged radium ions ( $\text{Ra}^+$ ), the square of the sin of the Weinberg angle  $\sin^2\theta_W$  can be extracted. This angle describes the mixing of the weak and the electromagnetic force in the Standard Model. Deviations of the Weinberg angle from the value expected in the Standard Model of particle physics could be due to physics beyond the Standard Model. An experiment like this is performed at the Van Swinderen Instituut of the RUG. The experiment will be performed in a single  $\text{Ba}^+$  ion. Thereafter the experiment will be carried out in a single  $\text{Ra}^+$  ion, because the expected effects are larger for  $\text{Ra}^+$ . The energy level diagrams for a  $\text{Ba}^+$  ion and a  $\text{Ra}^+$  ion are given in Fig. [1.1](#).

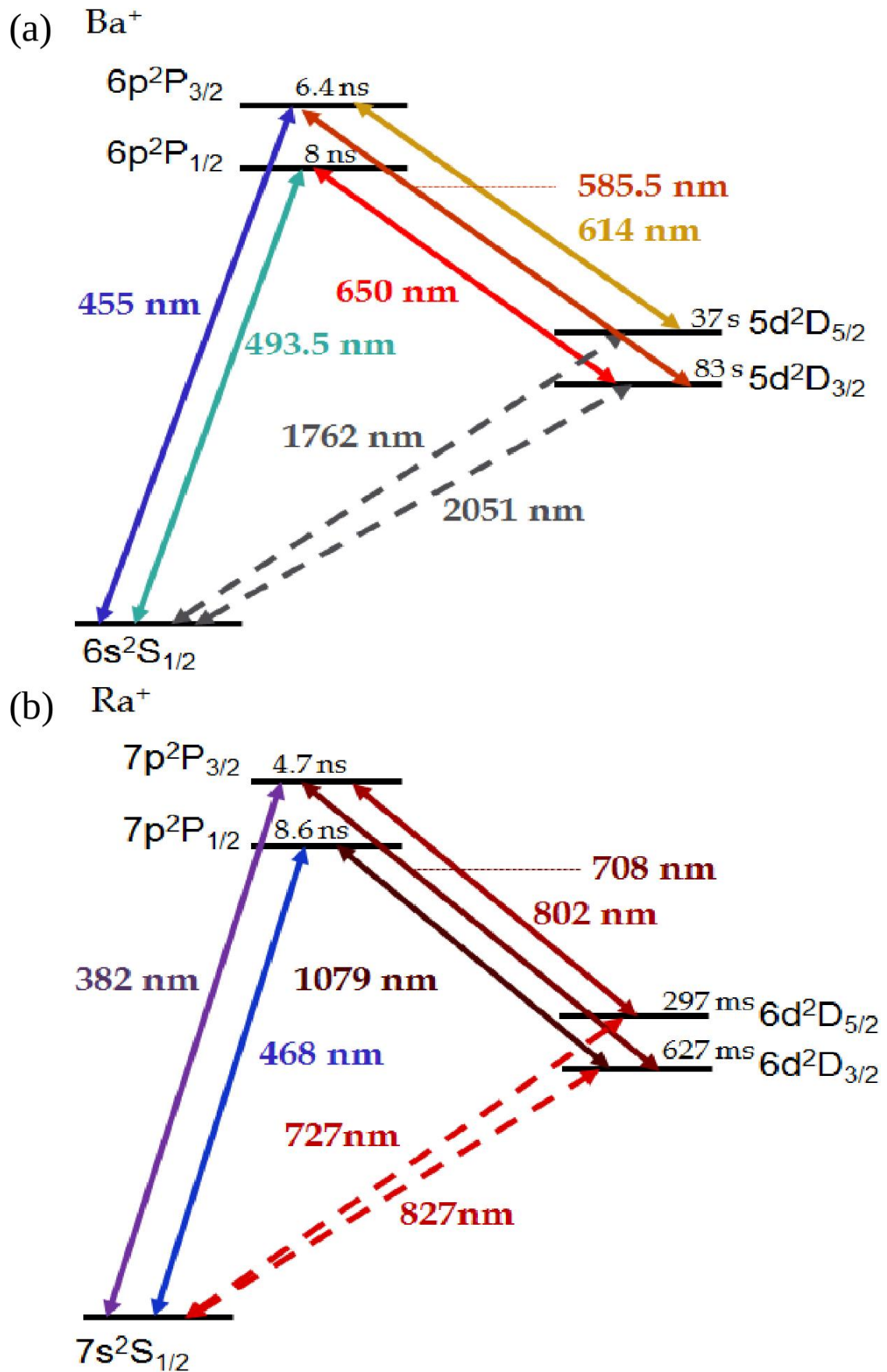


FIGURE 1.1: The energy level diagrams of  $\text{Ba}^+$  (a) and  $\text{Ra}^+$  (b). The two ions have a comparable subshell structure [1].

## 1.1 Atomic Parity Violation

The Standard Model is the theory, which describes three of the four fundamental forces in a coherent picture. It gives a very good description of the strong force, the electromagnetic force and the weak force. It is however incomplete. The fourth fundamental force, gravity, for example can not be described by the Standard Model. Other physics that is not covered is e.g. the existence of dark matter. Two main approaches are distinguished to search for physics beyond the Standard Model. Either new particles and interactions can be found directly in high energy experiments. The Higgs boson is a recent example of this [2, 3]. The number of these experiments is however limited, because of the high costs and the huge scale of these experiments. Another way to search for physics beyond the Standard Model is to perform high precision experiments at low energy scales. Deviations from the Standard Model would indicate its incompleteness. An example of this method is the search for Atomic Parity Violation (APV) [4].

There are discrete symmetries in the Standard Model. Among them are Parity (P), time reversal (T) and charge conjugation (C). Parity is the operation of space reflection. It can be described by the operator  $\hat{P}$ . Mathematically this means  $\hat{P}\vec{r} = -\vec{r}$ . It was common believe that parity was conserved by the three fundamental forces in the Standard Model. In 1956 Lee and Yang suggest that parity might be violated in the nuclear beta-decay [5]. Parity violation was found in the beta-decay of  $^{60}\text{Co}$  in 1957 by Wu. and co-workers [6]. Parity violation in atoms has been observed in several experiments. For example by Bouchiat et al. in 1977 [7]. Parity violation has also been report in the Bi atom by Barkov and Zoloterov in 1978 [8] and by Chu and Commins in the Tl atom in 1979 [9]. During the past decades several of these measurements were done. And APV was measured in several atoms. The most accurate results have been obtained with Cs atoms [10].

M.A. Bouchiat and C. Bouchiat showed that APV scales with the cube of the atomic number  $Z$  [11]. Recent work has proven that APV actually increases faster than with  $Z^3$ . It increase with an extra relativistic factor  $K_{rel}$ . The effect of this relativistic factor has been calculated and is shown in Fig. 1.2.  $\text{Ra}^+$  is the heaviest alkaline atom. Since radium ( $Z=88$ ) is heavier than cesium ( $Z=55$ ), the APV effect should be much larger in radium than in cesium. Therefore it is a promising atom for measuring APV. The APV effect has been calculated to be 50 times larger in radium than in cesium [12]. However,  $\text{Ra}^+$  is radioactive and therefore the experiment can be set up more efficiently with  $\text{Ba}^+$ .  $\text{Ba}^+$  has a similar valence electron structure as  $\text{Ra}^+$ . It is therefore a perfect candidate for debugging and testing the setup. By testing the experiment with  $\text{Ba}^+$ , agreement between calculations and experiments can be verified.

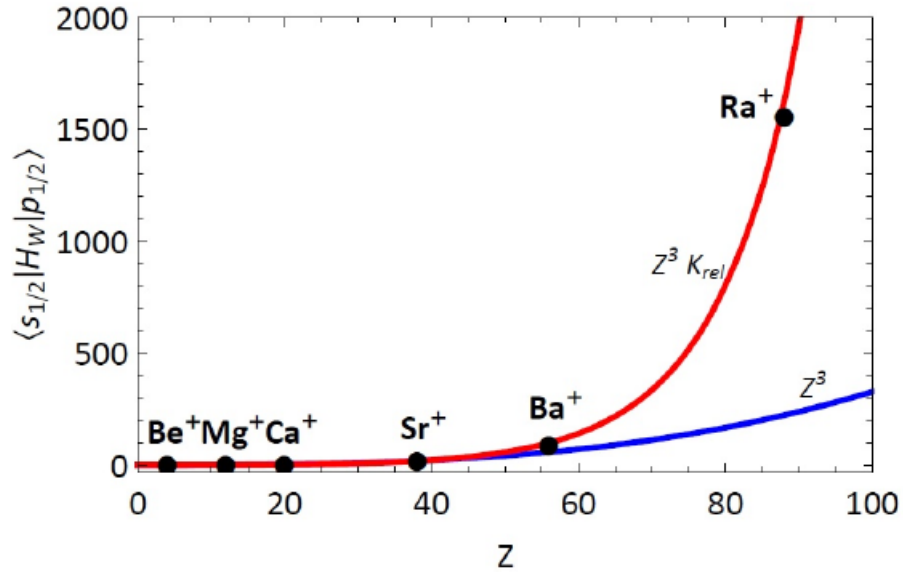


FIGURE 1.2: The scaling of the APV matrix element with atomic number  $Z$ . The lower line represents scaling with  $Z^3$ . The upper line represents scaling with  $Z^3$  taking the relativistic correction factor  $K_{rel}$  into account [12].

Parity can be violated in weak interactions. The EM interactions are mediated by the exchange of photons, the weak interactions by the exchange of  $W^\pm$  and  $Z^0$  bosons. A main difference between these two interactions, is that the photon is massless and the  $Z^0$  boson has a significant mass. Therefore the weak interaction is very short-ranged compared to the electromagnetic interaction. In the Standard Model, the electroweak interaction describes a combination of the electromagnetic interaction and the weak interaction [13]. Since the purely weak term is typically orders of magnitude smaller than the electromagnetic term it is difficult to detect. However the weak interaction can be well investigated by looking at the interference term between the EM and the weak interaction.

For a single  $\text{Ba}^+$  ion an APV signal can be obtained by measuring a weak interaction induced transition amplitude for electric dipole forbidden transitions. The  $6s\ ^2S_{1/2} - 5p\ ^2D_{3/2}$  transition is normally forbidden by selection rules for atomic transitions, e.g. in a dipole transition the parity must change. Since the two states of the transition have the same parity, an electric dipole transition (E1) is forbidden. The transition is however allowed through the weak interaction due to mixing of opposite parity states by the  $Z^0$  boson exchange. Such a transition is denoted by  $\text{E1}^{APV}$ . Quadrupole transitions due to electromagnetic interaction are allowed for the  $6s\ ^2S_{1/2} - 5p\ ^2D_{3/2}$  transition. The interference between these two interactions causes a light shift in the ion. By measuring the light shift, for a well chosen configuration of light fields, the electroweak interaction and thus the weak interaction can be investigated [4].

The electroweak interaction provides a measurement for the Weinberg angle  $\theta_W$ . This angle relates the strength of the coupling constants of the EM interaction and the weak interaction. It is given by

$$\sin^2\theta_W = \frac{e^2}{g_W^2}, \quad (1.1)$$

where  $e$  is the coupling constant of the EM interaction and  $g_W$  is the coupling constant of the weak force. The Weinberg angle  $\sin^2(\theta_W)$  can be measured. It depends on the energy scale. Fig. 1.3 shows  $\sin^2(\theta_W)$  as predicted by the Standard Model (the solid line). Deviations of  $\sin^2(\theta_W)$  from predictions of the Standard Model at low momentum transfer could be explained by e.g. dark Z-bosons. Three values for assumed masses of the dark Z-boson are given in the figure and are represented by the dashed lines. By investigating the Weinberg angle at low energy scales, the Standard Model can be tested and physics beyond the Standard Model can be searched for.

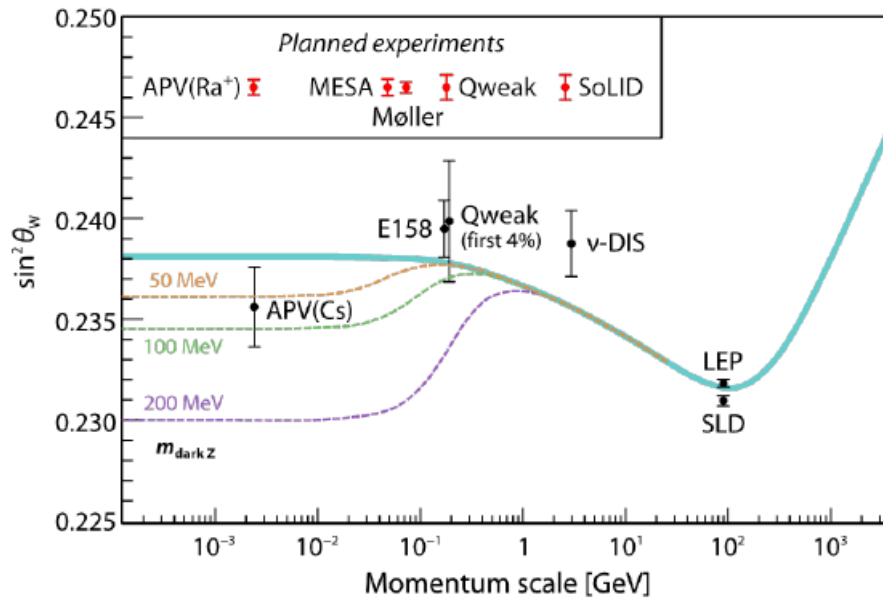


FIGURE 1.3: The expected value  $\sin^2\theta_W$  (Weinberg angle  $\theta_W$ ) as a function of the momentum scale. The dotted lines represent the expected values for  $\sin^2(\theta_W)$  for different masses of a possible dark Z boson [14, 15].

## 1.2 Light shift to measure Atomic Parity Violation

In this experiment the interaction of light with atoms is investigated. We employ light to create intense light fields, which can be on-resonant or off-resonant. On-resonant means that the light has the same wavelength as an atomic transition  $|1\rangle \rightarrow |2\rangle$ . This causes the atom to have a transition from state  $|1\rangle$  to state  $|2\rangle$ . State  $|2\rangle$  subsequently decays. This process continues, therefore there is an exchange in population by these two states called Rabi oscillation. Off-resonant high intensity light also interacts with atoms. The interaction between the laser field and the atom causes a shift in the energy levels of the atom. This effect is called "light shift". This shift happens because a changing electric field interacts with the atom. Therefore the effect is also called AC-stark shift. This is opposed to the Stark effect, which causes atomic states to split in several levels, due to the presence of an external static electric field. For a two level system the light shift is given by [1]

$$\Delta E = \pm \hbar \frac{\Omega^2}{4\delta}, \quad (1.2)$$

where  $\Omega$  is the Rabi frequency, and  $\delta = \omega_0 - \omega_L$  is the detuning of the laser light. From this formula can be concluded that the light shift scales as  $1/\delta$  with the detuning. And since  $\Omega \propto \sqrt{I}$  it scales linear with the intensity of the laser light. It also depends on the polarization of the laser beam with respect to the dipole moment of the atom [16]. The principle of the light shift can be seen in Fig. 1.4

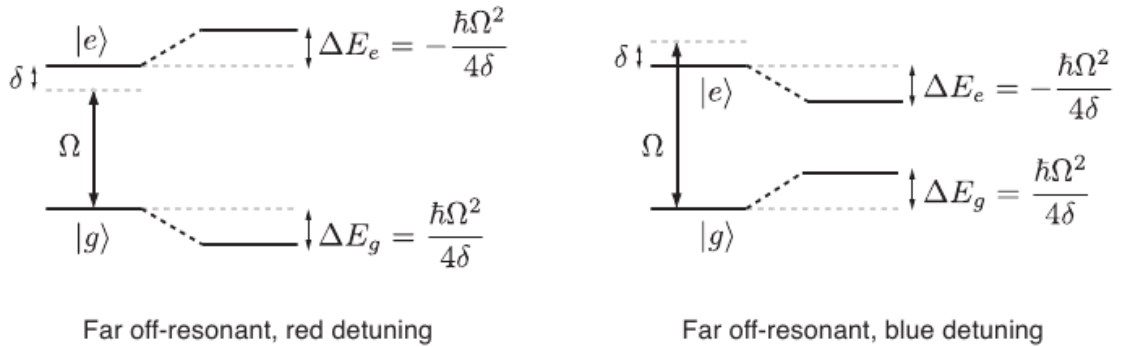


FIGURE 1.4: The principle of light shift for a two level system. The ground state and the excited state are light shifted due to off-resonant light [16].

## Chapter 2

# Experimental Setup

### 2.1 Concept of the experiment

In this experiment the light shift in a single trapped  $\text{Ba}^+$  ion is going to be measured. For this a single trapped  $\text{Ba}^+$  ion is exposed to off-resonant laser light. High precision laser spectroscopy is performed on the transition. This way the light shift can be measured and the Weinberg angle can be extracted.

Fig. 2.1 displays the experimental setup. A hyperbolic Paul trap is employed to trap a single  $\text{Ba}^+$  ion [17]. The trap is located in a vacuum chamber with a residual gas pressure of around  $10^{-11}$  mbar. An oven is used to produce barium atoms. This device consists of a hollow needle, filled with  $\text{BaCO}_3$  and Zr powder. By heating the needle, a beam of barium atoms is produced. Different lasers are part of the setup. There is a diode laser to photionize the barium atoms into  $\text{Ba}^+$  ions. The light from two lasers, a dye laser and a frequency doubled Ti:Sapphire laser, is used to cool the ion and to perform laser spectroscopy on the ion. A diode laser is used to search for the light shift in a single  $\text{Ba}^+$  ion. Light from a frequency comb is used to frequency lock light of the Ti:Sapphire laser to and to perform high precision laser spectroscopy. A Data Acquisition Program (DAQ) is used to collect data from the experiments. The DAQ includes of images from an EMCCD camera and a photo multiplier tube (PMT). The EMCCD camera is used to see an ion once it is trapped. The PMT collects photons.

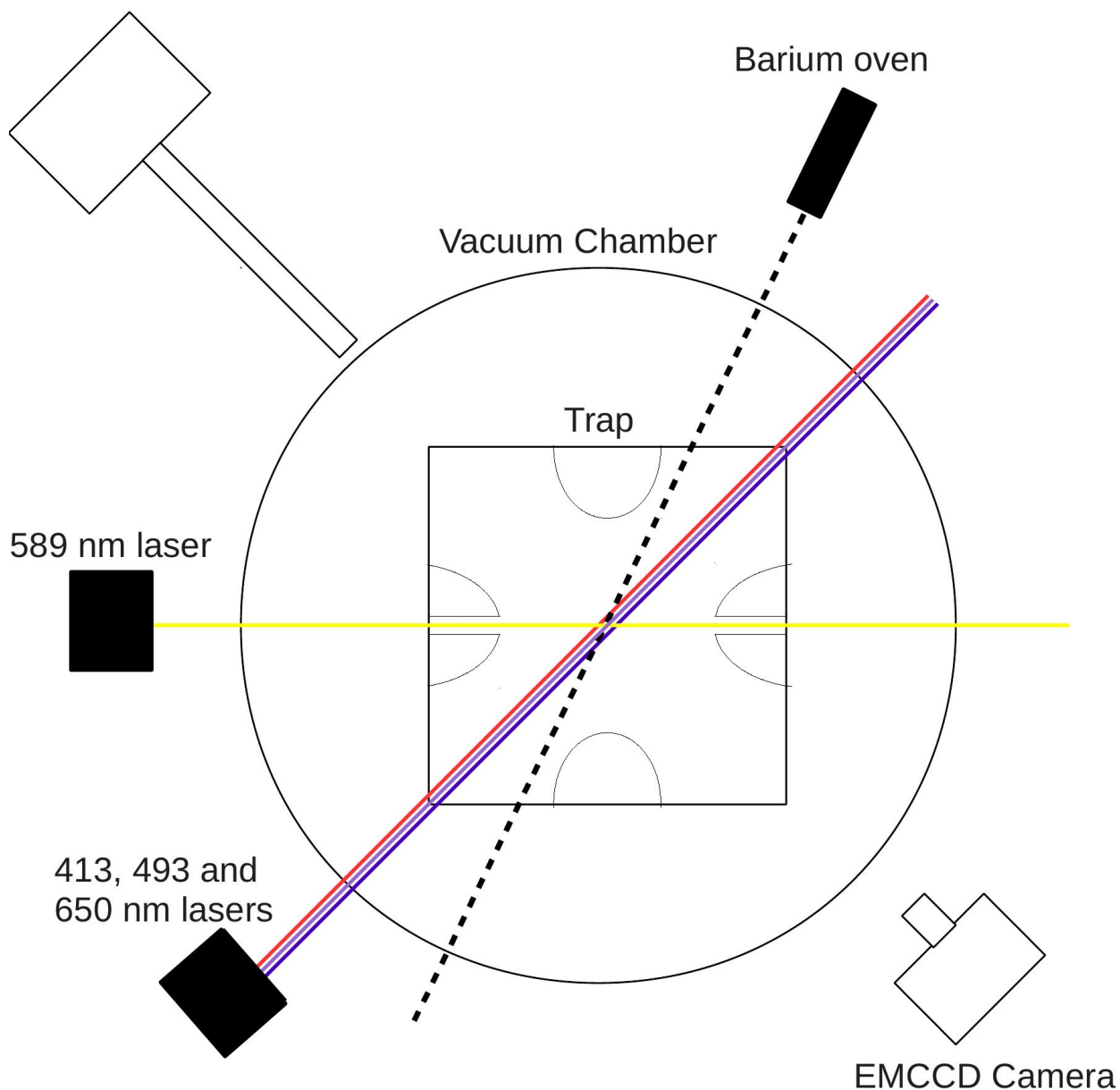


FIGURE 2.1: A schematic overview of the experimental setup. A hyperbolic Paul trap is used to trap  $Ba^+$  ions in the center of it. The trap sits inside a vacuum chamber. A resistively heated oven evaporates Barium atoms. They are photoionized to  $Ba^+$  ions by a laserbeam at a wavelength of 413.4 nm. Laserlight at a wavelength of 493.5 nm and 649.8 nm cools the  $Ba^+$  ions. This light also serves for laser spectroscopy. Laser light at a wavelength of 589 nm can induce a light shift in a single  $Ba^+$  ion. A photomultiplier tube (PMT) detects and counts photons. An EMCCD camera gives an image of a trapped  $Ba^+$  ion.

## 2.2 How to trap a single ion

It is crucial for the experiment to obtain a single ion and trap it. In section 2.2.1-2.2.5 we describe how to obtain a single ion.

### 2.2.1 Ion trap

A hyperbolic Paul trap is employed to trap ions. A hyperbolic trap works with dynamic electric fields to trap ions. If a particle is charged, it experiences a force in an electric field. The electric fields are set up in such a way that the motion of the ions are restricted to be inside the trap. The trap consists of a hyperbolic shaped ring and two end caps. These are the trap electrodes. A radiofrequency (RF) and a DC potential are applied between the ring and the end cap electrodes to create the electric trapping field. The net force with which they act on the ions pulls them to the center of the trap. Fig. 2.2 shows how the trap looks like. A detailed description the function principle of the trap can be found in [17].

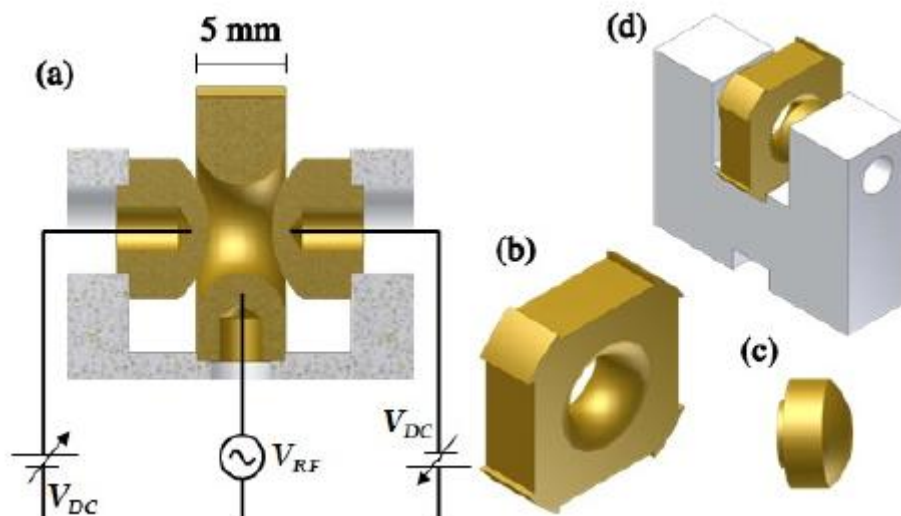


FIGURE 2.2: The hyperbolic Paul trap which is used to trap ions [17].

### 2.2.2 Ion source

The barium oven consists of a hollow needle. The needle is cut to a size of a diameter of 0.9 mm and a length of 40 mm. The needle is cleaned in an ultrasonic bath with an ethanol solution. After this the air is pumped out of the needle, and by doing so, the residual ethanol is removed. This needle is filled with a mixture of  $\text{BaCO}_2$  and Zr powder. It isn't filled till the top of the needle, to reduce the divergence of the beam.

The needle is then connected to a DC current source. It is mounted at the back end and somewhere before the top to a holder which is kept at room temperature. This leaves the tip of the needle cold, which reduces the divergence of the atomic beam. By driven a current of more than 5 A through the needle, the mixture of BaCO<sub>2</sub> and Zr powder is heated to a sufficiently high enough temperature to produce barium atoms. An atomic beam of barium atoms leaves the needle [17]. It is however hard to know whether barium atoms are coming out of the oven. To test whether barium atoms were coming out of the oven, several tests were performed.

### 2.2.3 Testing the oven in a vacuum chamber

If there are no barium atoms being produced by the oven, it is impossible to trap a Ba<sup>+</sup> ion. It is hard to see whether barium atoms are produced by the oven or not. Therefore tests have been performed to check the trap. A vacuum chamber was assembled, where the oven was put in. The sides of the chamber consisted of glass windows for vision on the trap. A roughing pump and a turbo pump were used to pump the residual gas pressure down to around 10<sup>-7</sup> mbar. The oven was connected to a power supply. By increasing the current passing through the oven in small steps, the voltage-current characteristics, the pressure in the chamber and the color of the oven were explored. The voltage-current characteristics of the oven can be seen in Fig. 2.3. The plot shows a curve which is not totally linear. This is what is expected for the oven, since the temperature rises in the oven. With an increasing temperature, the resistance in the oven increases. Since  $V = IR$  the voltage will increase faster than the current because of the double scaling. The plot seems to go through the origin which is as expected, since at a current of 0 A the voltage should be 0 V. The result of this measurement doesn't give a reason to believe that the trap isn't working.

By looking through the windows the colour of the mixture of BaCO<sub>2</sub> and Zr powder was inspected. When the mixture is glowing, the temperature is expected to be sufficiently high for barium atoms to be produced. The mixture started glowing around 6 A, so with this current the oven should work. From the pressure characteristics of the vacuum chamber there could not be concluded whether barium atoms were coming out or not. The pressure inside the vacuum chamber did rise, which is expected when barium atoms are produced. However, this could be due to chemical reactions inside the oven, or due to the rise of temperature inside the chamber.

### Current vs Voltage

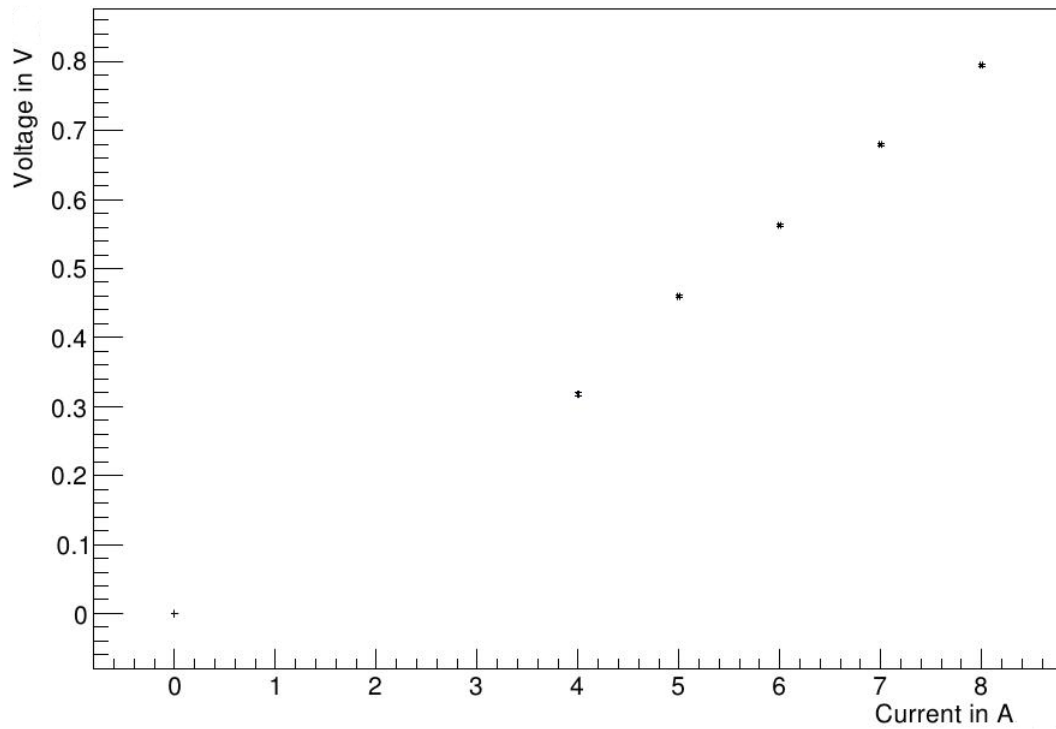


FIGURE 2.3: Current through the oven vs the applied voltage.

#### 2.2.4 Testing the oven with a laser

Barium atoms have a lot of different transitions from one energy state to another energy state. One of these transitions is used to identify barium atoms which are coming out of the oven. The  $6s^2 \ ^1S_0 - 6s6p \ ^1P_1$  transition from a barium atom is at a wavelength of 553.7 nm [18]. A laser is passed through to go the trap and to cross with the beam of barium atoms. This laser is tuned to the transition at 553.7 nm. If barium atoms are exposed to this resonant light, the  $6s^2 \ ^1S_0 - 6s6p \ ^1P_1$  will be driven. Subsequently, the atoms fall down to the  $6s^2 \ ^1S_0$  ground state and send out a photon in a random direction. This principle causes the laserlight to scatter if it passes a beam of barium atoms. The PMT can collect these photons. If the PMT is set to collect photons of 553.7 nm it can be tested whether the oven works, by collecting scattered light with the PMT. If the PMT doesn't give a signal, the barium oven doesn't work and a new oven should be assembled and put into the setup.

We performed the test and the results are given in Fig 2.4. There is a peak in the PMT count rate, which is induced by the fluorescence of the barium atoms. This means that the oven is producing barium atoms. From these results the angle of the laser beam with respect to the atomic beam can be calculated. The peak which is seen in the spectrum

from the PMT is broadened due to the Doppler effect, because the atomic beam has a velocity. A relationship between the full width half maximum  $\Delta\nu_D$  (the width of the peak where the intensity is half of it's maximum) and the velocity of the particles in the beam is given by

$$\Delta\nu_D = \frac{2\nu_0}{c} \sqrt{\frac{2k_B T \ln 2}{m}}, \quad (2.1)$$

where  $\nu_0$  is the frequency of the atomic transition and  $m$  is the mass of the particles in the beam. Since  $\nu_0 = c/\lambda$  and  $k_B T = (1/2)mv^2$ , we obtain the formula

$$\Delta\nu_D = \frac{2}{\lambda} \sqrt{\frac{2}{3} v_z^2 \ln 2}, \quad (2.2)$$

where  $v_z = v \sin \theta$  is the velocity of the atomic beam along the axis of the laserbeam and  $\theta$  is the angle between the atomic beam and a line perpendicular to the laser beam. Rewriting this formula gives an angle  $\theta$  of

$$\theta = \sin^{-1} \left( \frac{\Delta\nu_D \lambda}{2v \sqrt{\frac{2}{3} \ln 2}} \right). \quad (2.3)$$

We determined  $\Delta\nu_D$  to be  $(140 \pm 20)$  MHz from Fig. 2.4. Using the values,  $\lambda = 1107$  nm,  $\Delta\nu_D = (140 \pm 20)$  MHz and  $v = (350 \pm 50)$  m/s we obtain an angle  $\theta$  of  $\theta = 18^\circ \pm 2^\circ$ .

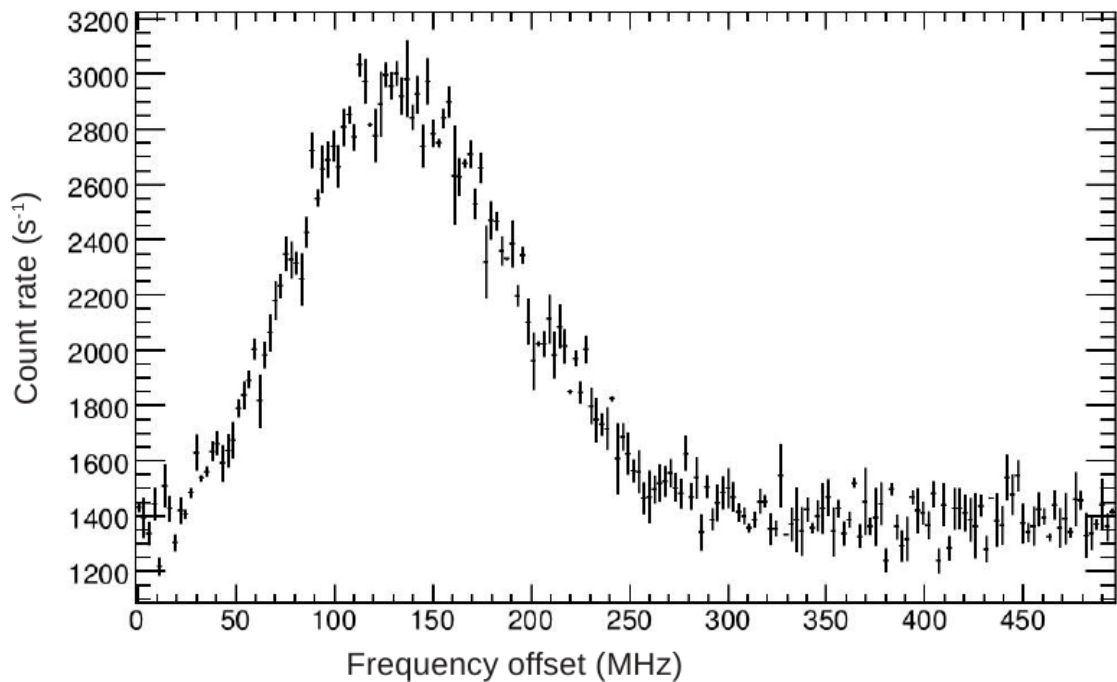


FIGURE 2.4: The count rate of the PMT vs the offset of the barium test laser operating at 1107 nm. The spectrum from the PMT has been created by scanning the laserlight over a frequency range of 500 MHz. The full width half maximum due to Doppler broadening is determined to be  $(140 \pm 20)$  MHz.

### 2.2.5 Creating one single ion

After a beam of barium atoms is obtained, the atoms can be ionized by a laser [19]. The laser which is used has a wavelength of 413.4 nm. Light with this wavelength drives a two-photon ionization with a resonant intermediate state in Ba. The first photon couples the  $6s^2 \ ^1S_0$  ground state with the  $5d6p \ ^3D_1$  excited state. The second photon excites the electron above the ionization threshold. By doing this a  $\text{Ba}^+$  ion is created. The two-photon process to ionize the barium atoms is shown in Fig. 2.5

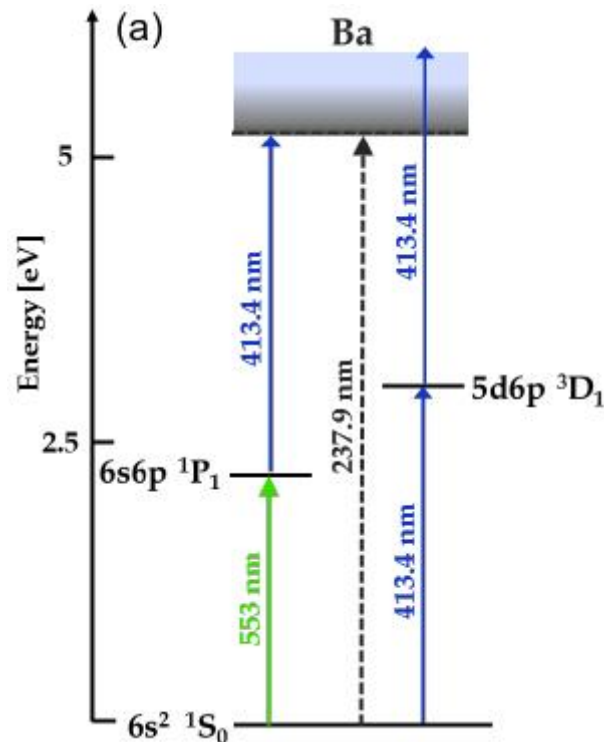


FIGURE 2.5: The two-photon ionization in barium which is used to photoionize the barium atoms [19].

## 2.3 Vacuum Chamber

In order to perform high precision experiments, the residual gas pressure in the trap needs to be as low as possible. Collisions with the residual gas in the vacuum chamber, where the trap is in, reduce the lifetime of a trapped ion. The trap is mounted on a flange which is attached to a vacuum chamber. The chamber is brought down to a pressure of an order of magnitude of  $10^{-11}$  mbar. This is achieved in three steps. The chamber is pumped down by a roughing pump to reach a pressure of  $10^{-4}$  mbar. Then a turbo pump is used to pump the chamber down to a pressure of around  $10^{-8}$  mbar. After that an ion pump is used to reach pressures of an order of magnitude of  $10^{-11}$  mbar. This kind of

pressure can only be obtained by continuously heating the chamber and running the ion pump for a few days. The vacuum chamber is heated for two main reasons. It increases the velocity of the particles inside the chamber, so the chance of capturing particles with the ion pump is higher. It heats the particles which are residing at the surfaces of the chamber enough to a high enough energy to pass the energy barrier which keeps them on the surface. Now these particles can be captured by the ion pump.

## 2.4 Lasers

Lasers are a crucial part of the experiment. The setup contains a photoionization laser, two lasers to cool the ion, a laser for the light shift and a laser to test whether barium atoms are coming out of the oven. A frequency comb is used as a high precision light source to frequency lock a laser to. In sections 2.4.1-2.4.2 ion cooling and frequency doubling, are explained. Section 2.4.3 explains the principle of a frequency comb. Sections 2.4.3-2.4.7 explain which lasers are used and what their role is in the experiment.

A laser is a source of light which emits a coherent light bundle of a high intensity and a single wavelength. Laser action consists out of three main principles [20]. Stimulated emission in a gain medium, population inversion of the gain medium and an optical resonator. A source of light, or optical gain is needed in the laser. This is called the lasing or gain medium. The gain is the result of stimulated emission of an electronic or molecular transition. An electronic or molecular transition from a higher level energy state to a lower level energy state can happen in two ways, by spontaneous emission or by stimulated emission. Spontaneous emission is the process where a photon is spontaneously emitted into a random direction, if a transition occurs from a higher level to a lower level. This effect produces fluorescence light. The frequency of the light depends on the specific transition. If a medium has multiple transitions, photons with different wavelengths will be created. For lasers, stimulated emission is the main emission process which is used. This is the process where a transition from a higher energy level to a lower level is induced by a photon [21]. The photon which stimulated this process and the photon emitted have the same frequency, the same direction and will be in phase with each other. A laser uses this principle to create light of a single wavelength. In a thermal equilibrium however, there are far more electrons in a ground state than in an excited state. This causes the absorption of photons to dominate over spontaneous emission. That is why population inversion is needed to create laserlight.

Population inversion means that the higher level has a greater population than the lower level. Most lasers achieve this by using a 4-level system. Level 1 is the ground state,

level 4 is the highest level state and level 2 and 3 are two levels in between. The ground state is pumped by an external energy source and excites to state 4. Subsequently the state relaxes relative fastly into state 3. After that they decay from state 3 to state 2. This is a relative slow process. This is the decay where laser light is emitted. The decay from state 2 to state 1 is again a fast process. Because the decay from state 2 to state 1 is much faster than the decay from state 3 to state 2, population inversion is easily achieved. Once population inversion is achieved, stimulated emission can be the dominant process in a laser.

The last main part of a laser is an optical resonator, also called a cavity. The cavity causes a positive feedback mechanism. Without a resonator, a photon can only go through the gain medium one time, thus reducing the chance of stimulated emission. Therefore the gain is low. The cavity causes photons to go through the gain medium multiple times. This way a high gain can be achieved. The cavity usually consists of an arrangement of mirrors. One end of the cavity is made as reflective as possible and the other end of the cavity is made semi-transmissive. Laserlight can "leak out" of the semi-transmissive mirror and laser light is produced. The optical cavity also acts as a wavelength selector [20].

### 2.4.1 Ion cooling with lasers

Lasers can be used to cool an ion, which is reducing the velocity of an ion [22, 23]. A barium ion (in the experiment barium is used, but the laser cooling principle is the same for other atoms) has several electric dipole transitions. These electric dipole transitions each have their own resonance frequency. Each time a scattering event occurs, the ion receives a momentum impulse  $\hbar\vec{k}$  by absorbing a photon, where  $\vec{k}$  is the wave vector of the photon. The ion receives another momentum impulse by reemitting a photon. The process can be seen in Fig. 2.6. Since this is a random event, with equal chances in all directions, on average this adds nothing to the momentum of the ion. The average effect on the ion is therefore that the velocity is changed by [23]

$$\Delta\vec{v} \cong \frac{\hbar\vec{k}}{M}, \quad (2.4)$$

where  $M$  is the mass of the ion and  $\vec{v}$  is the velocity of the ion. Therefore, when the ion is moving towards the laser beam, so  $\vec{v} \cdot \vec{k} < 0$ , its velocity will be reduced, provided that  $|\vec{v} + \Delta\vec{v}| < |\vec{v}|$ . The ion will be irradiated by monochromatic laser light near the resonance frequency. To cool the ion, the laser light has a frequency slightly lower than that of the resonant dipole transition. Therefore, the ion will most likely be scattered by a photon, when its resonant frequency is Doppler shifted towards the frequency of the

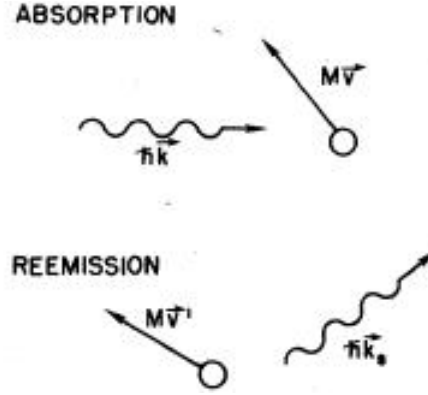


FIGURE 2.6: The scattering process explained. First a photon is absorbed, then it is reemitted in a random direction [23].

laser light, so when  $\vec{v} \cdot \vec{k} < 0$ . This explains how the cooling process itself works.

There is a minimum temperature which can be reached due to residual heating effects. Every scattering event has a minimum recoil energy of  $R = (\hbar k)^2/2M$ . This means that an ion can never be cooled to a temperature of 0 K using this method. The total energy difference of the ion per absorbed photon is,

$$\Delta E = \hbar \vec{k} \cdot \vec{v} + R. \quad (2.5)$$

The ion is cooled if  $\hbar \vec{k} \cdot \vec{v} < -R$  [23]. The highest deceleration of the ion is obtained by using high light intensities, because a high intensity light causes a higher absorption rate. The maximum deceleration is limited, because high intensity lasers increase the absorption rate, but also increase the stimulated emission rate. For a stimulated emission process, the ion emits a photon with the same direction as that of the laser beam, the net effect on the momentum will therefore be zero. The deceleration saturates at  $\vec{a}_{max} = (1/M)(\Delta \vec{p}/\Delta t) = \hbar \vec{k} \gamma / 2M$ . This gives a minimum temperature, called the Doppler limit of

$$T_{min} = \frac{\hbar \Gamma}{2k_B}, \quad (2.6)$$

where  $\Gamma$  is the natural linewidth of the transition and  $k_B$  is the Boltzmann constant. For  $\text{Ba}^+$  the Doppler cooling limit is 470  $\mu\text{K}$ .

### 2.4.2 Second harmonic generation

A technique called second harmonic generation [24], also known as frequency doubling, is used in the experiment. It is used for the diode laser, which tests the oven and it is used for the Ti:Sapphire laser, which cools the ion. Frequency doubling is the process where two photons of the same frequency "create" a photon of two times this frequency. Light

with frequency  $\omega$  is led into a frequency doubling medium, usually a crystal, and light with frequency  $2\omega$  comes out. This is a process of nonlinear optics. Nonlinear optics, is optics described in a nonlinear medium. A nonlinear medium is a medium in which the dielectric polarization is not linear proportional to the electric field. The nonlinear response can cause an exchange of energy between electromagnetic fields of different frequencies (or two fields of the same frequency in this case). This only happens for high intensity electric fields, e.g. lasers. For second harmonic generation, a part of the energy of light with wavelength  $\omega$  is converted to light with frequency  $2\omega$  by propagating through a frequency doubling medium. For efficient second-harmonic generation, it is required that there is a phase matching condition  $\Delta k = 0$  between the incoming and the outgoing laserbeam, where  $k$  is the phase shift. The condition  $k^{2\omega} = 2k^\omega$  follows from this. Since  $k^\omega \propto n^\omega$  this gives the condition  $n^{2\omega} = n^\omega$ , where  $n$  is the index of refraction. This means that the index of refraction for light of the incoming laser beam and the index of refraction of light from the frequency doubled beam should be the same. For normally dispersive material, the index of refraction increases when  $\omega$  increases. An ordinary wave and an extraordinary wave have a different index of refraction for a given  $\omega$ . Ordinary waves are waves with it's electric field perpendicular to the optical axis of the crystal, extraordinary waves are waves with it's electric field parallel to the optical axis. The index of refraction for ordinary and extraordinary waves changes at a different pace with a changing  $\omega$ . This means that under certain circumstances it is possible to satisfy  $n^{2\omega} = n^\omega$  an ordinary and an extraordinary are used. The index of refraction also depends on the angle  $\theta$  between the propagation direction of the laser beam and the crystal optic axis,

$$\frac{1}{n_e^2(\theta)} = \frac{\cos^2\theta}{n_o^2} + \frac{\sin^2\theta}{n_e^2}. \quad (2.7)$$

From this relation, the angle  $\theta_m$  can be calculated at which the optimal power from the frequency doubled beam is obtained.

$$\sin^2(\theta_m) = \frac{(n_o^\omega)^{-2} - (n^{2\omega_o})^{-2}}{(n_e^{2\omega})^{-2} - (n_o^{2\omega})^{-2}}, \quad (2.8)$$

where the subscripts o and e stand for ordinary and extraordinary. When it is known how the index of refraction scales with the frequency for ordinary and extraordinary beams, the best angle of the beam with the optical axis of the crystal can be calculated [24].

A phase matching condition should be achieved. There should be a proper phase relationship between the interacting waves along the propagation axis. The phase matching condition depends on the temperature of the frequency doubling crystal as well. The

crystal should have the right temperature to yield the best results for frequency doubling. A more detailed description of nonlinear effects in media can be found in [24].

### 2.4.3 Frequency comb

Light from a frequency comb is used to frequency lock the Ti:Sapphire laser. A detailed description of a frequency comb can be found in e.g. [25]. A frequency comb is a light source whose frequency spectrum consists of a series of equally spaced modes. Frequency combs can be produced by the pulse train of a mode-locked laser. A mode-locked laser is a laser which produces pulses of light of very short duration. The laser is locked by establishing a fixed-phase relationship between all the longitudinal modes of the laser. The pulses are in the order of magnitude of femtoseconds. The idea behind this principle is that a regular spaced train of pulses corresponds to a comb in the frequency domain. This can be explained by first introducing the carrier envelope phase. An optical pulse can be described as an envelope superimposed on a carrier wave. The envelope function is given as  $E(t)$ . This function describes how the laser pulses propagate. The function is superimposed on a continuous carrier wave with frequency  $\omega_c$ . The electric field of the pulse can be written as

$$E(t) = \hat{E}(t)e^{i\omega_c t}. \quad (2.9)$$

The phase shift between the peak of the envelope and the closest peak of the carrier wave is called  $\phi_{ce}$ . In general, the group velocity and the phase velocity are not the same, so this phase shift will change as the pulse propagates in a laser cavity. Due to this, successive pulses being emitted from a mode-locked laser are different. In the frequency domain this produces a spectrum in the form of a comb, because at certain discrete values of the frequency, the interference between the pulses is constructive. Since  $t = 1/f$ , the short duration of the pulses means that the frequency bandwidth of the comb spectrum will be high. Since the pulses are repetitive in time, the comb spectrum will have equal spacing between each comb line. The spacing is coupled to the repetition rate of the laser. This principle is shown in 2.7.

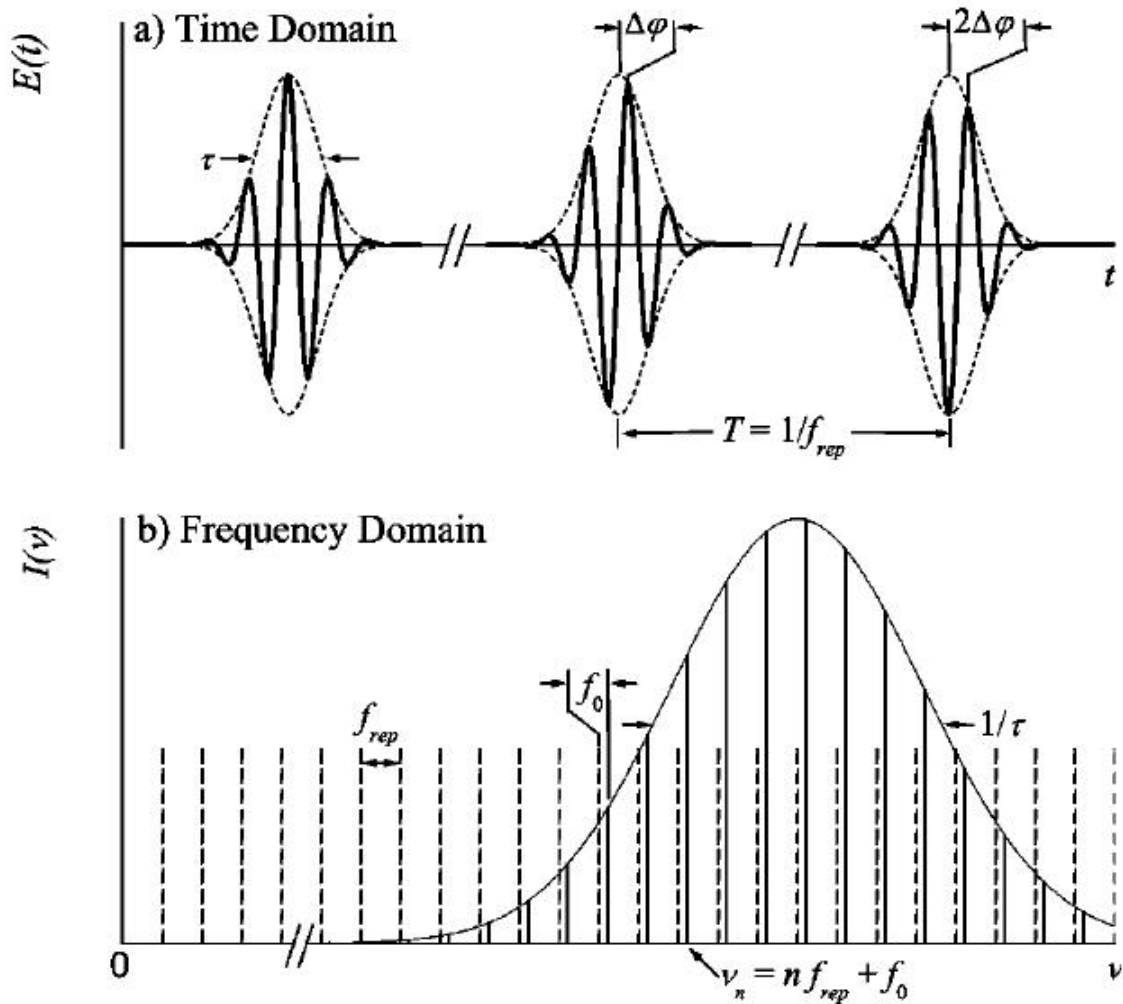


FIGURE 2.7: The principle of how a frequency comb is formed in the frequency domain. A train of short (fs) pulses (a) can be Fourier decomposed into a comb of equidistant frequencies (b) [25].

The frequency of a comb line is given by,

$$f_n = f_0 + n f_{rep}. \quad (2.10)$$

Here  $f_0$  is the frequency comb offset,  $f_r$  is the spacing of the frequency comb and  $n$  is an integer which gives the number of the comb line [25].

A frequency comb is very useful in making frequency measurements. If the phase difference and the repetition time between pulses are locked to a clock, very precise measurements can be performed. These measurements are performed by comparing the light of a laser to the closest comb line. In this experiment a frequency comb is used measure the wavelength of the Ti:Sapphire laser and to frequency lock it to the frequency comb. The laser is locked by comparing the laserlight with light from the frequency comb, by detuning the laser light or detuning the offset of the frequency comb from a specific

line. When the two wavelengths match, a beatnote signal can be seen. An example of a beatnote signal is given in Fig. 2.8. If such a signal is obtained, the laser can be locked to the frequency comb and the frequency comb can be used to scan the laser.

In the experiment, a femtosecond frequency comb with a spacing of 250 MHz is used (Model FC1500/075 from Menlo Systems).

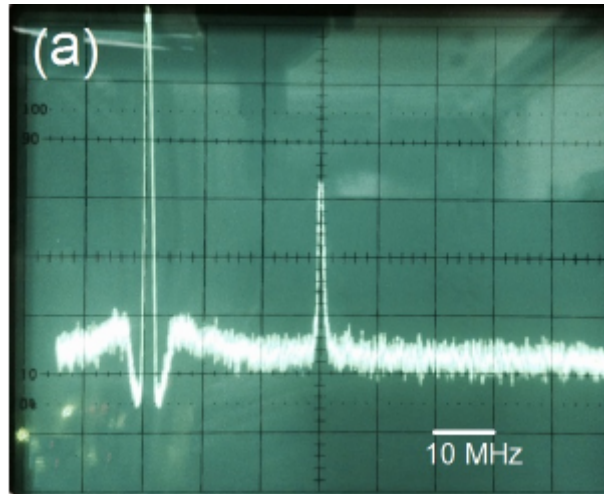


FIGURE 2.8: An example of a beatnote signal as recorded on a rf spectrum analyzer [17].

#### 2.4.4 The barium test laser

One of the lasers, is a laser which is used to test whether barium atoms are coming out of the oven or not. It is a semiconductor diode laser (Toptica LD1120-0300-1) operating at a wavelength of 1107.4 nm. This light is frequency doubled by a LBO crystal to 553.7 nm. Light with this wavelength drives the transition  $6s^2 \ ^1S_0 - 6s6p \ ^1P_1$  transition in a barium atom.

A semiconductor diode laser has a semiconducting material as it's gain medium. An electric current flows through a p-i-n structure. When electrons and holes recombine in such a medium, energy is released in the form of photons. This effect can happen spontaneous, or it can be induced by photons, comparable to stimulated emission. Optical feedback is achieved by the stimulated emission process. The use of a laser resonator makes optical amplification possible. A laserdiode can be described by two main characteristics, a threshold current and a power slope. There is a threshold current, because the gain of the laser must be higher than the losses of the resonator for a laser to work. This laser has a threshold current of 44(1) mA as determined from Fig. 2.9. The power slope of a diode laser is supposed to be linear. The laser was tested and the slope is linear as can be seen in Fig. 2.9. The slope of this laser is  $\Delta P/\Delta I = 1.84W/A$

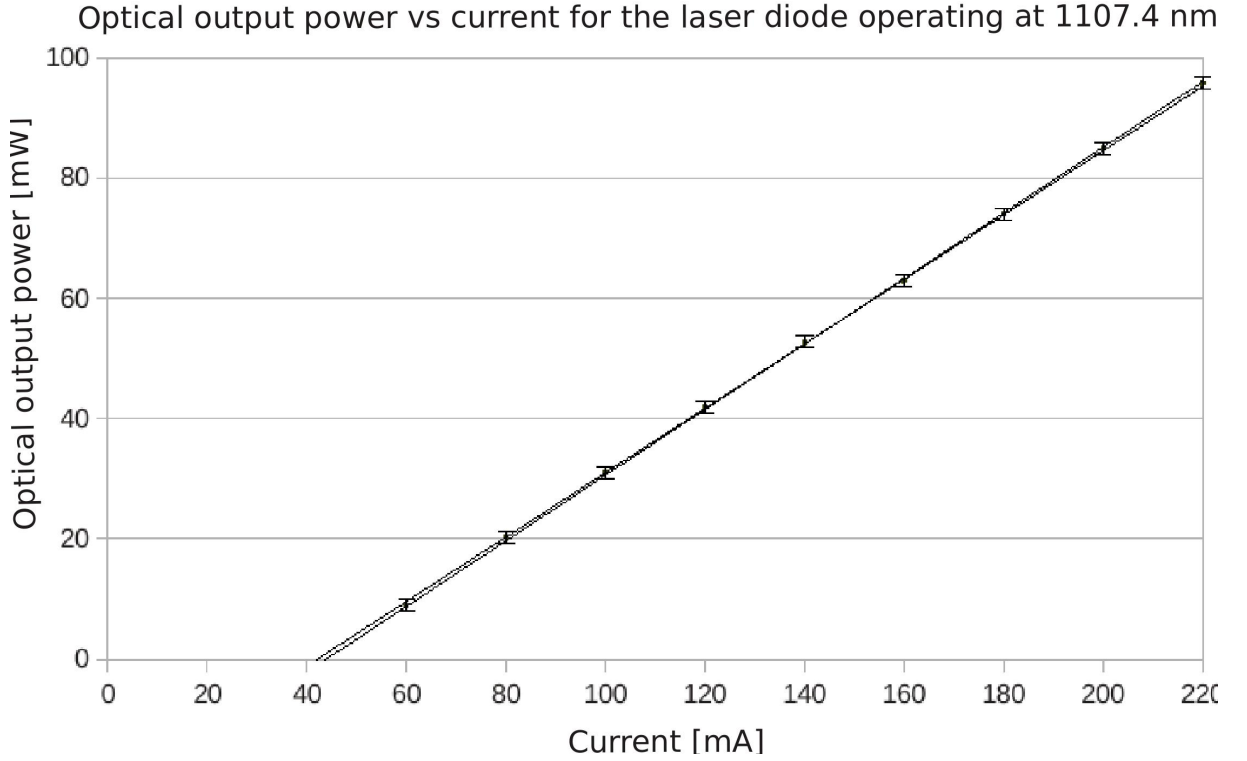


FIGURE 2.9: Power vs current for the semiconductor laser diode (Toptica LD1120-0300-1) operating at 1107.4 nm. The lasing threshold for this device is found at 44(1) mA.

#### 2.4.5 Light shift laser

The laser used to induce a light shift in a single  $\text{Ba}^+$  ion is a semiconductor laser diode. This is a tunable laser with an integrated frequency doubling mechanism. The wavelengths which are used for this experiment are 588-590 nm. The maximum output power of the laser for these wavelengths is 1000 mW. The laser is on a different optical table as the experimental setup. It is brought to the room where the trap is in by coupling it to a single mode optical fiber. The maximum output power at the exit of the fiber is around 500 mW. The transition which is mainly light shifted by this laser is the  $5d^2D_{3/2} - 6p^2P_{3/2}$  transition [26]. This transition is 585.530 nm as can be seen in Fig. 1.1. The detuning of the laser with respect to this transition is in the order of magnitude of a few nm. With sufficiently high laser power a light shift should be measurable.

#### 2.4.6 The cooling and detection lasers

Two lasers are used to cool the ion and to perform laser spectroscopy. To cool the ion, two transitions in the  $\text{Ba}^+$  ion are used, the  $6s^2S_{1/2} - 6p^2P_{1/2}$  transition and the  $5d^2D_{3/2} - 6p^2P_{1/2}$  transition. These transitions and their wavelengths are indicated in Fig. 1.1. They are 493.55 nm and 649.87 nm. To cool the ion, the wavelengths of the

two lasers need to be detuned a small amount above this value.

For the 493.55 nm transition a single frequency Ti:Sapphire Laser is used. This is a single-frequency laser with a wavelength of 987 nm. To produce light with a wavelength of 493.5 nm this light is doubled using a MgO doped PPNL second harmonic generation crystal. This crystal needs to be heated to the right temperature to acquire the phase matching condition. This laserlight light is brought to the barium lab by coupling it to a single mode fiber. To have a good control over this laser it is locked to the frequency comb. By doing this a control of the order of 1 MHz is possible. When the laser is locked to the frequency comb, a beatnote as in Fig. 2.8 will be seen. By locking the laser, it can be controlled by the frequency comb and precise measurements can be performed [17].

For the 649.87 nm transition a dye laser is used. A dye laser is a laser which uses an organic dye as lasing medium. This laser is locked to an iodine locked diode laser. What this means is that first a diode laser is locked to a specific line of iodine. Iodine can be used for this, because the transitions of molecular  $I_2$  are known very precisely. The wavelength of the light from the diode laser is referenced to a specific transition of the  $I_2$ . This transition is known in an accuracy of 1 MHz [27]. The dye laser is locked to the iodine locked diode laser. The laserlight from the dye laser is brought from the laser lab to the barium lab with a single mode optical fiber [17].

#### 2.4.7 Photoionization laser

For photionizing the barium atoms, a semiconductor diode laser (Thorlabs DL5146-101S) is used. The laser operates at a wavelength of 413.4 nm and drives the two photon transition as can be seen in Fig. 2.5. It's beam is directed opposite to the lasers beam at 493.5 and 649.9 nm, by using wavelength selective mirrors in the optical path after the trap. The laser is only used for the start of the experiment to ionize the ions.

## 2.5 Data acquisition

The data acquisition (DAQ) is a crucial part in the setup. It is used to collect the data from the experiment. The DAQ consists of two main components. A Photo Multiplier Tube (PMT) and an Electron Multiplying Charge Coupled Device (EMCCD) camera. A PMT is a device which detects photons. Illuminating the ion with the cooling lasers excites it to the  $6s\ ^2P_{1/2}$  state. Either by the  $6s\ ^2S_{1/2} - 6p\ ^2P_{1/2}$  transition or by the  $6d\ ^2D_{3/2} - 6p\ ^2P_{1/2}$  transition. When the ion is in this state it can fall down to the  $6s\ ^2S_{1/2}$  state or the  $6d\ ^2D_{3/2}$  state. If it falls down to the  $6s\ ^2S_{1/2}$  state, a photon with wavelength of 493.5 nm is sent out, as can be seen in Fig. 1.1. The PMT has a wavelength filter built into it. This filter is set to only collect photons with a wavelength of 490-500 nm. Once one or multiple ions are trapped they give a signal to the PMT by sending out photons. An example of such a signal can be seen in Fig. 2.10.

The EMCCD is a camera, which provides an image of an ion once it is trapped. It is a digital camera which is capable of detecting single photon events. Therefore a single ion can be seen by the camera. An example of this can be seen in Fig. 2.10 [17].

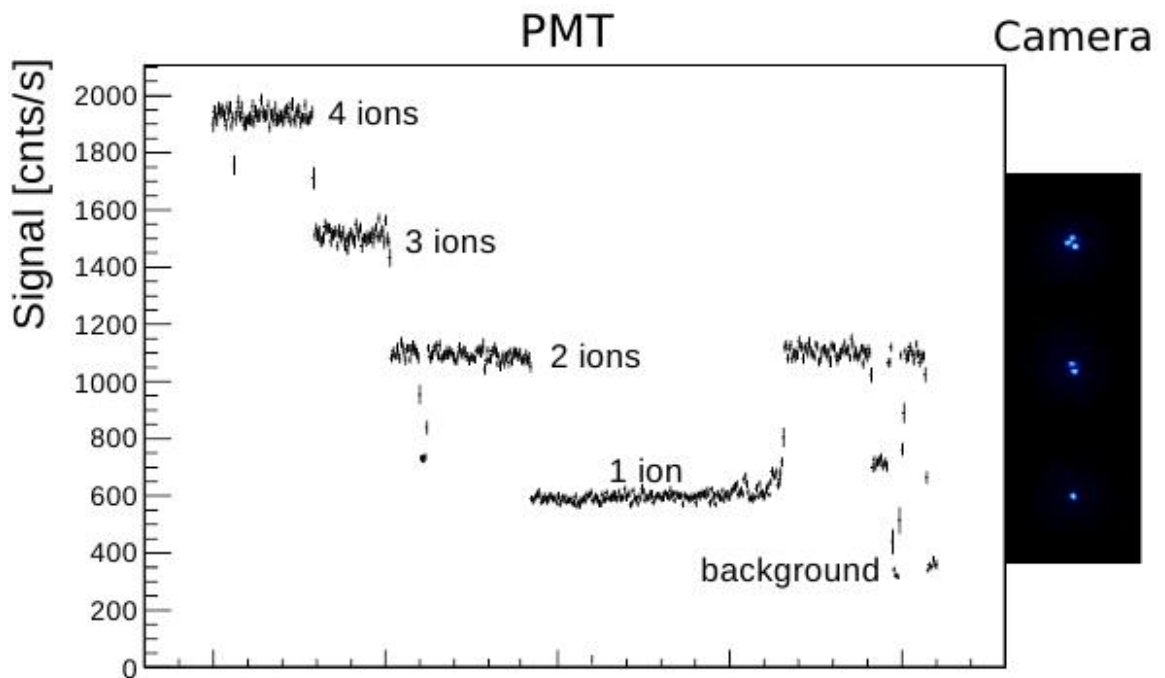


FIGURE 2.10: The photomultiplier count rate of the fluorescence signal for 4, 3, 2 and 1 ions as a function of time. We also see the background count rate. Right is an example of images of 3, 2 and 1 stored ions from the EMCCD [17].

## Chapter 3

# Measurement plan for the experiment

An understanding of what to look for in the data from the DAQ is crucial to find a light shift. The different parameters involved in the experiment and how they affect the light shift measurements needs to be known.

The light shift is going to be measured by scanning the frequency of one of the cooling lasers over an interval, while the other laser stays fixed at one frequency. A scan like this gives produces a spectrum from the PMT like the one seen in Fig. 3.1. The dip in the middle is called a Raman dip. A Raman dip occurs due to two photon transitions from the  $6s\ ^2S_{1/2}$  state to the  $5d\ ^2D_{3/2}$  state. A two photon transition occurs when the detuning of the two cooling lasers is the same, so when  $\delta_r = \delta_g$ , where  $\delta_r$  is the detuning of the 649.9 nm laser and  $\delta_g$  is the detuning of the 495.5 nm laser. This principle can be seen in Fig. 3.2. The population in the  $6p\ ^2P_{3/2}$  is minimal when two photon transitions occur. The fluorescence of the ion is therefore minimal, because the 495.5 nm transition can not occur if the ion is not in the  $6p\ ^2P_{3/2}$  state.

Once a spectrum is obtained by scanning a laser, there will be a fast way to search for the light shift. This is to fix the scanned laser at a point in the spectrum where the slope of the Raman dip is the steepest. Turning on the light shift laser and looking at changes of the PMT count rate could indicate be due to a light shift of the  $Ba^+$  ion.

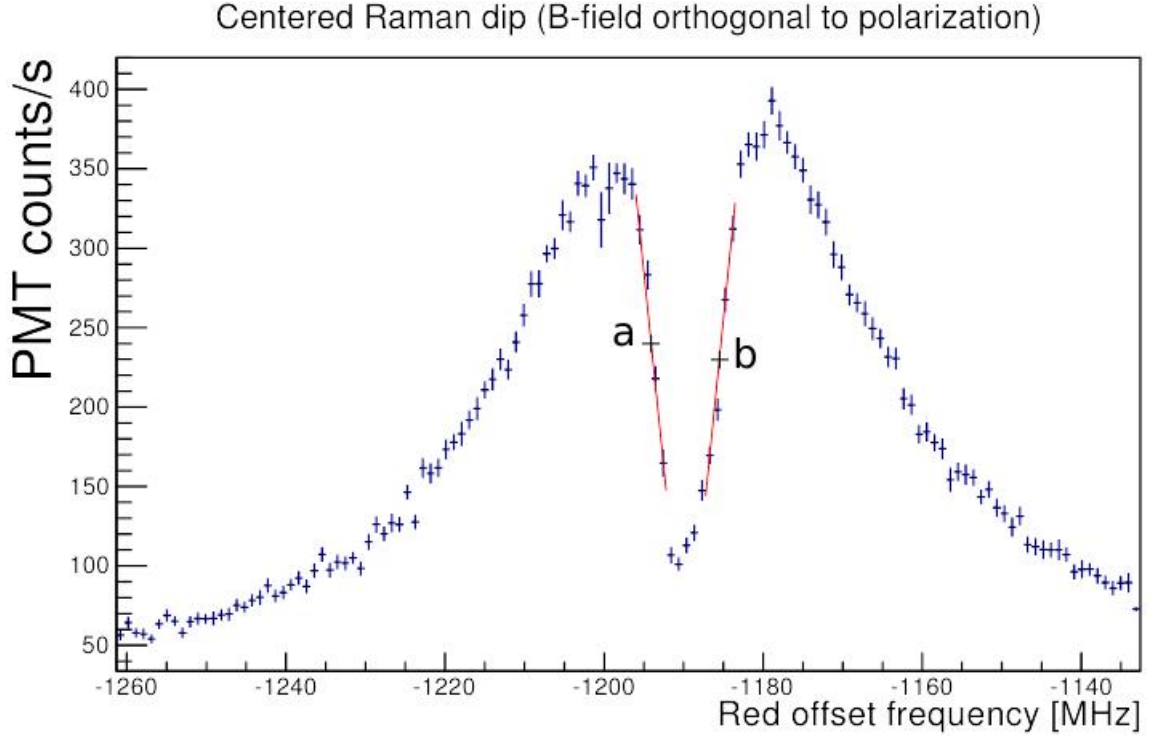


FIGURE 3.1: An example of a scan of the red laser. A Raman dip can be seen in the middle. The two points denoted by A and B are the points where the slope of the Raman deep is the steepest and measurements can be performed there [28].

### 3.1 Different parameters

Good knowledge about how different parameters in the experiment influence the measured light shift are required to do high precision measurements. Two parameters on which the light shift depends are the laser power and the detuning of the laser with respect to a transition. Good control over the spectrum from the PMT is also required to do high precision experiments. To know how this parameters change the spectrum, two things can be performed. Predictions can be made, by presenting physical arguments. After these predictions are made they can be tested by changing the parameters and see wether the change in the spectrum agrees with the made predictions. In sections 3.1.1-3.1.5, a list of different parameters is given. It is discussed how they affect the light shift and how they are expected to change the spectrum given by the PMT.

The transtion in a single  $\text{Ba}^+$  ion which will have the biggest light shift due to the light shift laser is the  $5d \ ^2D_{3/2}$ - $6p \ ^2P_{3/2}$  transition. This transition has a wavelength of 585.530 nm. The light shift laser has a wavelength of 588-590 nm. The laser can be detuned 3.470-5.470 nm with respect to this specific transition. The "light shift laser" has a maximum power of around 500 mW once it reaches the trap. The beam waist of the laser is  $35(4) \ \mu\text{m}$ .

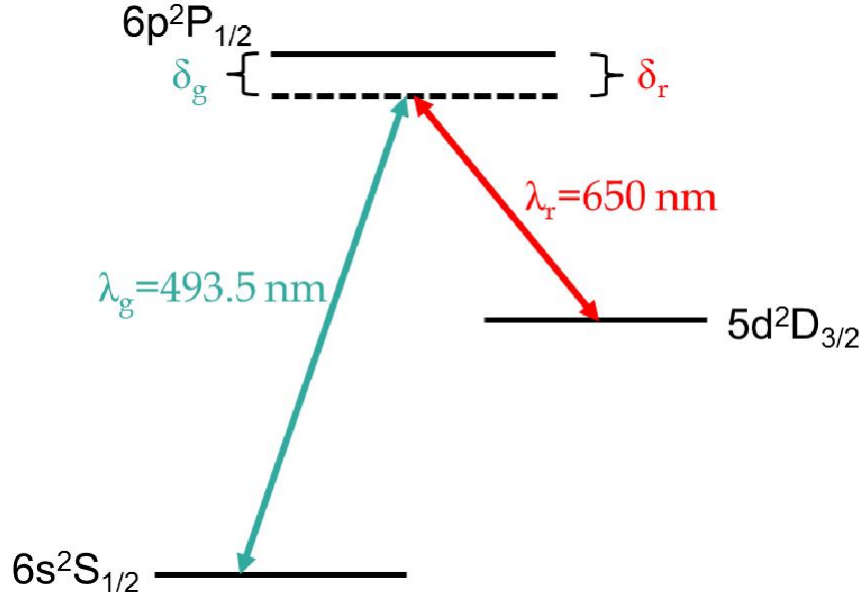


FIGURE 3.2: The principle of a two photon transition. Because this transition happens, the fluorescence from the  $6p^2P_{1/2} - 6s^2S_{1/2}$  transition is lost [17].

### 3.1.1 Laser power

Three lasers are used for performing laser spectroscopy and measuring the light shift. The two cooling lasers, which are used to perform the laser spectroscopy and the light shift laser. The two cooling lasers do not influence the light shift of the  $5d^2D_{3/2} - 6p^2P_{3/2}$  transition on first order. They, however, do influence the spectrum from the PMT. Higher intensity for these lasers might mean a steeper slope in the Raman dip, because more photons can be collected when the laser intensity is higher. It will also mean that the PMT collects more background light due to scattering of the lasers inside the trap. These effects should be investigated by looking at the spectrum from the PMT for a few different laser powers of the cooling lasers.

The light shift scales linear with light intensity ( $\Delta \propto P$ ). Therefore, the light shift laser should have a power as high as possible. The light shift laser has a maximum output power of 500 mW. A high laser power has a drawback as well. High intensity laser light can cause off-resonant atomic transitions. In this case, the  $5d^2D_{3/2} - 6p^2P_{3/2}$  transition. If this transition occurs, two things can happen. The  $\text{Ba}^+$  ion can fall to the  $6s^2S_{1/2}$  state and return to the cooling cycle, or it can fall back to the metastable  $5d^2D_{5/2}$  state. This is called shelving. If the ion is in this metastable state it is no longer present in the cooling cycle and no fluorescence is seen. Spectroscopy is impossible with a shelved ion, so the shelving rate should be balanced with the size of the light shift.

Off resonant transitions occur, because the line shape of an atomic line has a Lorentz profile. The Lorentz profile for an atomic line is given by.

$$L(\omega - \omega_0) = \frac{\Gamma/2\pi}{(\omega - \omega_0) + (\Gamma/2\pi)^2} \quad (3.1)$$

Where  $\Gamma$  is the natural linewidth given by  $1/\tau$ ,  $\omega_0$  is the angular frequency of the resonant transition and  $\omega$  is the angular frequency of the laser light. Normalizing this function, so setting  $L(0) = 1$  gives the following normalized Lorentz profile

$$L(\omega - \omega_0) = \frac{1}{1 + 4 \left( \frac{\omega - \omega_0}{\Gamma} \right)^2} \quad (3.2)$$

This normalized Lorentz function can be coupled with the absorption probability per second of monochromatic light with frequency  $\omega$  for a specific transition

$$B\rho(\omega) = \frac{A_{21}}{2} \left( \frac{I}{I_{sat}} \right), \quad (3.3)$$

Here  $I$  is the intensity of the laser light given by

$$I = \frac{2P}{\pi\omega_0^2}, \quad (3.4)$$

$I_{sat}$  is the saturation intensity of the atomic line given by

$$I_{sat} = \frac{2\pi hc\Gamma}{\lambda^3}. \quad (3.5)$$

Therefore, the absorption rate for off resonant laserlight of a specific frequency and intensity is given by [29].

$$R = B\rho(\omega)L(\omega - \omega_0) = \frac{\frac{A_{21}}{2} \left( \frac{I}{I_{sat}} \right)}{1 + 4 \left( \frac{\omega - \omega_0}{\Gamma} \right)^2}. \quad (3.6)$$

In this work the absorption rate for the  $5d^2D_{3/2} - 6p^2P_{3/2}$  transition has been calculated (see Table 3.1).

### 3.1.2 Laser detuning

The three lasers can be detuned from their respective transitions. Detuning the cooling lasers will not change the light shift, but it might change the form of the spectrum from the PMT. If the cooling lasers are detuned too far, the signal to the PMT might get smaller. The slope of the Raman dip could differ for a different detuning of the 495.5 nm laser. This is why for a few different detunings of the 495.5 nm laser, the spectrum

should be investigated.

The light shift scales with the detuning as  $\Delta \propto 1/\delta$ . This means that for the highest possible light shift to be measured, the light shift laser should be set to be detuned to an as small as possible value. For a smaller detuning however, the absorption chance of a photon by the resonant transition increases with  $\delta^2$ . Since this effect scales quadratically and the light shift scales linear, the laser power should be as high as possible and the detuning should be adjusted to obtain an acceptable shelving rate.

### 3.1.3 Field gradients

The field gradients of the laser light of the light shift laser and the position of the ion with respect to it. Laser has a Gaussian beam profile. A Gaussian beam is a beam whose electric fields and intensity distributions are described by a Gaussian function. The maximum intensity is at the center of the beam. If the ion is not at the center of the beam, but at a sideband, the intensity of the laser light will be a lower, so the light shift will be lower as well. To measure the largest light shift, the ion should therefore be at the center of the laser beam.

### 3.1.4 Magnetic fields

Magnetic fields play an important role in the experiment. The main reason for this is the Zeeman effect. This is the effect where an atomic line is split into several components in the presence of a static magnetic field. The effect is analogous to the Stark effect, which is the splitting of an atomic line in the presence of a static electric field. In the presence of Zeeman splitting, there are multiple Raman dips in the spectrum due to several close lying states. For an accurate measurement of the light shift, the Zeeman splitting should be as low as possible. This can be achieved by making the direction of the magnetic field orthogonal to the polarization of the blue laser.

The best value for the strength of the magnetic field is determined in previous experiments, using this setup. A few different strength for the magnetic field can however be tested to see whether it is possible to obtain a better spectrum (steeper slope in the Raman dip) to measure the light shift.

### 3.1.5 Polarization

It is very important to know which effect the polarization of the laser beams has on the spectrum from the PMT and on the light shift of the Ba<sup>+</sup> ion. Electromagnetic waves (light) are polarized if the waves oscillates with a direction perpendicular to the direction of the wave. There are three ways electromagnetic waves can be polarized. Linear, circular or elliptical.

Linear polarized light are electromagnetic waves whose electric field vectors oscillate in one direction. The strength of the electric field changes over time. Circular polarized electromagnetic wave are wave whose electric field strength does not change over time, only the direction does. The direction of the electric field changes over time in a circular way. Elliptical polarization is a combination of circular and linear polarization. The direction and the strength of the electric field change over time. It is called elliptical polarization, because the tip of the electric field vector describes the motion of an ellipsis over time.

It is important to know how each laser should be polarized for optimal results. The 495.5 nm laser should be linear polarized and the direction should be perpendicular to the magnetic field, because this reduces the effect of Zeeman splitting and therefore a spectrum with a nice Raman dip can be produced. The 649.9 nm laser is circular polarized.

The light shift laser has specific requirements for the polarization. To know what this requirements are, the physics behind the light shift must be known. A light shift is obtained by the interference between an E2 quadrupole transition, driven by the EM interaction and an E1<sup>APV</sup> transition, driven by the weak force. To obtain the largest light shift, these two effects have to be maximized.

A linear polarized laser field can be described by

$$\vec{E}(\vec{r}, t) = \frac{1}{2}[\vec{E}(\vec{r})exp(-i\omega_L t) + c.c] \quad (3.7)$$

The propability of an APV dipole transition is proportional to the amplitude of the field. The ion should therefore be localized at the top of a standing wave to maximize this effect. Therefore the ion should be located at a top of a standing wave of the light shift laser. The E2 quadrupole transition propability is at a maximum if the field gradient is at a maximum. Therefore the ion must be localized at a node of the 495.5 nm laser. For the maximum affect of the light shift, which scales with the interference term ( $E1^{APV} \cdot E2$ ) the ion must be simutinaeously in a node of the 495.5 nm laser and at the top of the light shift laser [30]. The light shift laser must be polarized perpendicular to the 495.5 nm. These conditions can be seen in Fig. 3.3.

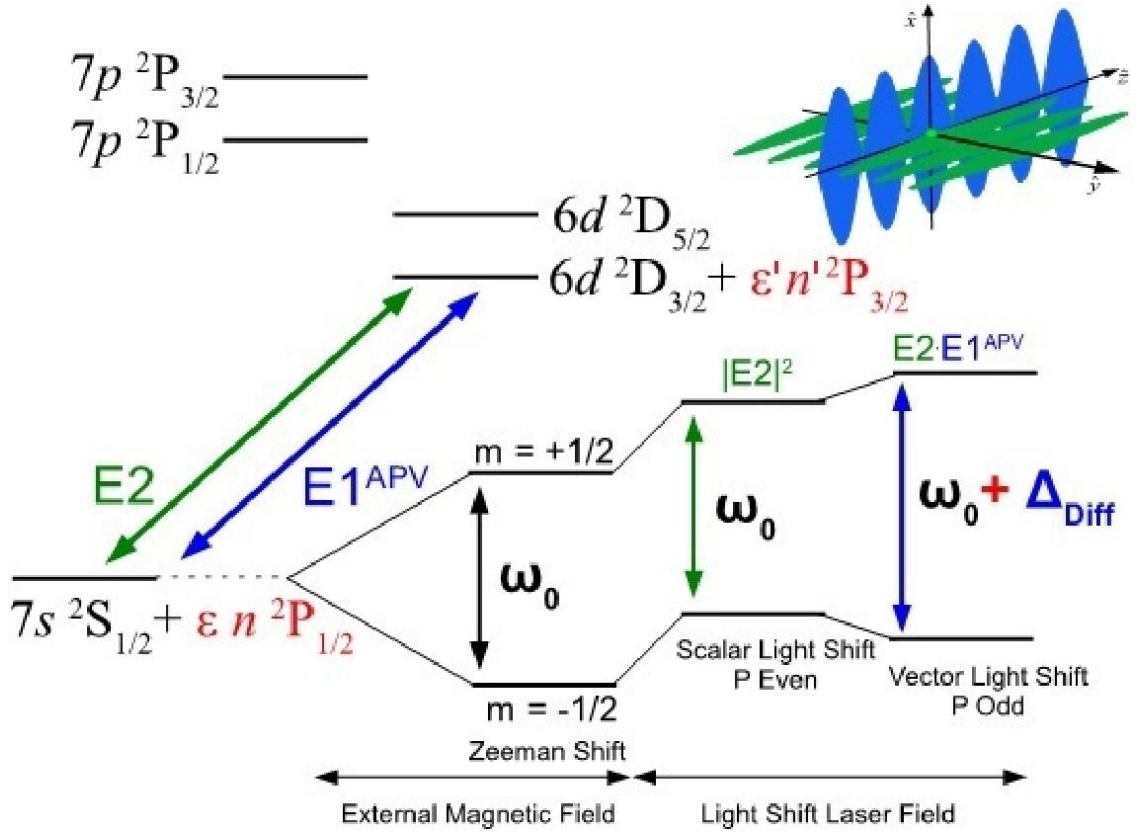


FIGURE 3.3: The principle of an APV measurement using a single  $\text{Ra}^+$  ion. For a  $\text{Ba}^+$  it is the same idea. At the right above corner can be seen how the "light shift laser" and the 495.5 nm laser (we plan to do this with light at  $2.05 \mu\text{m}$ ) should be polarized to yield a maximum result for  $E1^{APV} \cdot E2$ , [17].

### 3.2 Measuring a light shift

Once the parameters described above are investigated and it is known how they affect the spectrum from the PMT and the light shift, the actual light shift measurements can be performed. In the assumption of a two level-level system and optimal polarization of the laser beam, the light shift in a single  $\text{Ba}^+$  ion is calculated [26]. The light shift for a two-level system is given by

$$\Delta\omega = \frac{\Delta E}{\hbar} = \pm \frac{\Omega^2}{4\delta} \quad (3.8)$$

The actual change in frequency is then given by

$$\Delta\nu = \frac{\Delta\omega}{2\pi} \quad (3.9)$$

It is calculated that for a laser power of 2 W, a beam waist of  $46 \mu\text{m}$  and a laser wavelength of 589 nm, so a detuning of 3.47 nm, the light shift for the  $5d \ ^2D_{3/2} - 6p \ ^2P_{3/2}$  transition is  $\Delta\nu = 3.6(4) \text{ MHz}$  [26].

Because the scaling of the light shift with the intensity and the detuning of the laser beam is known, the light shift for a laser beam with a beam waist of  $35 \mu\text{m}$  can be calculated. The scaling of the intensity with the beam waist is given in equation 3.4.

The light shift per Watt, for a beam waist of  $35 \mu\text{m}$  and a detuning of  $3.47 \text{ nm}$  is therefore:

$$\Delta\nu/W = 3.6 \text{ MHz} * \frac{(46\mu\text{m})^2}{(35\mu\text{m})^2} * \frac{1}{2W} = 3.1 \frac{\text{MHz}}{W}.$$

The light shift mainly depends on the intensity of the laserlight and the detuning of the laserlight. An unwanted effect called shelving, however scales with the light intensity and detuning as well. Because this effect scales quadratically with the detuning and only linear with the laser power, the laser power should be as high as possible and the detuning should be adjusted to reach a good enough signal to noise ratio. A table for a laser power of  $500 \text{ mW}$  and a few different detunings is given. Here is used that  $A_{21} = 6.0 * 10^6 \text{ s}^{-1}$  [31] for eq. 3.3 .

TABLE 3.1: The light shift and shelving rate for different detunings and a laser power of  $500 \text{ mW}$ . The light shift has been calculated [26]. The shelving rate has been calculated using eq. 3.6.

Laser wavelength (nm)	Detuning (nm)	Light shift (MHz)	Shelving rate ( $\text{s}^{-1}$ )
588	2.47	2.2(3)	0.036
588.5	2.97	1.8(2)	0.025
589	3.47	1.6(2)	0.018
589.5	3.97	1.4(2)	0.015
590	4.47	1.2(2)	0.011

# Chapter 4

## Conclusion

### 4.1 Conclusion

This work has been performed in the context of the measurement of Atomic Parity violation in single trapped heavy alkaline earth atoms. The experiment is conducted in the Fundamental Interaction group of the Van Swinderen Institute of the University of Groningen.

The setup of the ion trapping apparatus is described in [17]. During this thesis several optimizations of the experimental setup were performed in order to prepare for light shift measurements on a single trapped  $\text{Ba}^+$  ion. The oven has been tested and we conclude that a barium atom beam is produced from the oven. With the new trap setup, ion signals have not yet been observed. Possible problems could be that the ionization laser is not working properly i.e. at the correct wavelength. This has been excluded by observing the absorption of the  $6s^2 \ ^1S_0 - 5d6p \ ^3D_1$  transition in barium, which is used to photoionize the barium atoms. It was observed that the wavelength meter calibration was off by 17 GHz, which is about 100 linewidths. Further the trap may not function as desired. This is presently investigated. Once the problem with the setup is discovered,  $\text{Ba}^+$  ions can be trapped as they could be in previous versions of the setup. After a single  $\text{Ba}^+$  ion is trapped and the experiment with barium is optimized, the light shift in radium is going to be measured. This should yield for better results and perhaps even the discovery of a dark Z boson.

# Bibliography

- [1] Gouri Shankar Giri. *Radium ion spectroscopy towards atomic parity violation in a single trapped ion*. PhD thesis, 2011. Relation: <http://www.rug.nl/> Rights: University of Groningen.
- [2] Serguei Chatrchyan, Vardan Khachatryan, Albert M Sirunyan, A Tumasyan, W Adam, E Aguilo, T Bergauer, M Dragicevic, J Erö, C Fabjan, et al. Observation of a new boson at a mass of 125 gev with the cms experiment at the lhc. *Physics Letters B*, 716(1):30–61, 2012.
- [3] Georges Aad, T Abajyan, B Abbott, J Abdallah, S Abdel Khalek, AA Abdelalim, O Abdinov, R Aben, B Abi, M Abolins, et al. Observation of a new particle in the search for the standard model higgs boson with the atlas detector at the lhc. *Physics Letters B*, 716(1):1–29, 2012.
- [4] E Norval Fortson and LL Lewis. Atomic parity nonconservation experiments. *Physics Reports*, 113(5):289–344, 1984.
- [5] T. D. Lee and C. N. Yang. Question of parity conservation in weak interactions. *Phys. Rev.*, 104(1):254–258, 1956.
- [6] Chien-Shiung Wu, Ernest Ambler, RW Hayward, DD Hoppes, and R Pl Hudson. Experimental test of parity conservation in beta decay. *Physical review*, 105(4):1413, 1957.
- [7] C Bouchiat. Parity violation in atomic processes. *Journal of Physics G: Nuclear Physics*, 3(2):183, 1977.
- [8] L. M. Barkov and M. S. Zolotarev. Observation of parity non-conservation in atomic transitions. *Jetp Lett.*, 27(6):357–361, 1978.
- [9] R Conti, P Bucksbaum, S Chu, E Commins, and L Hunter. Preliminary observation of parity nonconservation in atomic thallium. *Physical Review Letters*, 42(6):343, 1979.

- 
- [10] CS Wood, SC Bennett, D Cho, BP Masterson, JL Roberts, CE Tanner, and CE Wieman. Measurement of parity nonconservation and an anapole moment in cesium. *Science*, 275(5307):1759–1763, 1997.
- [11] M. A. Bouchiat and C. Bouchiat. Parity violation induced by weak neutral currents in atomic physics .1. *J. De Physique*, 35(12):899–927, 1974.
- [12] Liselotte Willemina Wansbeek. *Atomic parity violation in a single radium ion*. PhD thesis, 2011. Relation: <http://www.rug.nl/> Rights: University of groningen.
- [13] Sheldon L Glashow. Partial-symmetries of weak interactions. *Nuclear Physics*, 22(4):579–588, 1961.
- [14] Hooman Davoudiasl, Hye-Sung Lee, and William J Marciano. Muon  $g-2$ , rare kaon decays, and parity violation from dark bosons. *Physical Review D*, 89(9):095006, 2014.
- [15] KS Kumar, Sonny Mantry, WJ Marciano, and PA Souder. Low energy measurements of the weak mixing angle. *arXiv preprint arXiv:1302.6263*, 2013.
- [16] J.A. Sherman. *Single barium ion spectroscopy: light shifts, hyperfine structure, and progress on an optical frequency standard and atomic parity violation*. PhD thesis, 2007.
- [17] Mayerlin Nuñez Portela. *Single ion spectroscopy in preparation of an atomic parity violation measurement in Ra+*. PhD thesis, 2015.
- [18] Subhadeep De. *Laser cooling and trapping of barium*. PhD thesis, 2008. Relation: <http://www.rug.nl/> Rights: University of Groningen.
- [19] G. Leschhorn, T. Hasegawa, and T. Schaetz. Efficient photo-ionization for barium ion trapping using a dipole-allowed resonant two-photon transition. *Applied Physics B*, 108(1):159–165, 2012. ISSN 0946-2171.
- [20] S. Orazio. *Principles of lasers*. Springer, 4th edition, 1998. ISBN 9781441913012.
- [21] Albert Einstein. Strahlungs-emission und absorption nach der quantentheorie. *Deutsche Physikalische Gesellschaft*, 18:318–323, 1916.
- [22] Theodor W Hänsch and Arthur L Schawlow. Cooling of gases by laser radiation. *Optics Communications*, 13(1):68–69, 1975.
- [23] D. J. Wineland and W. M. Itano. Laser cooling of atoms. *Phys. Rev. A*, 20(4):1521–1540, 1979.
- [24] A. Yariv. *Quantum Electronics*. Wiley, 1988. ISBN 9780471609971.

- 
- [25] J. Ye and S.T. Cundiff. *Femtosecond Optical Frequency Comb: Principle, Operation, and Applications*. Kluwer Academic Publishers / Springer Norwell, MA, 2005. ISBN 9780387237916.
- [26] J. Hussels. Light shift in  $Ba^+$  and  $Ra^+$  ions. 2014.
- [27] Simon Gerstenkorn and Paul Luc. Atlas du spectre d'absorption de la molecule d'iode 14800-20000  $cm^{-1}$ . *Paris: Editions du Centre National de la Recherche Scientifique (CNRS), 1978*, 1, 1978.
- [28] T. Meijknecht. Light fields for measuring light shifts in  $Ba^+$  ions, 2014.
- [29] S.N. Thakur D.K Rai. *Atom, laser and spectroscopy*. PHI, 2010. ISBN 9788120339569.
- [30] Norval Fortson. Possibility of measuring parity nonconservation with a single trapped atomic ion. *Physical review letters*, 70(16):2383, 1993.
- [31] NIST database. [www.nist.gov](http://www.nist.gov).
- 

**Acknowledgments.** This work has been conducted at the Van Swinderen Institute of the University of Groningen. The parity project is supported by the Dutch Stichting voor Fundamenteel Onderzoek der Materie (FOM) in the framework of the research programmes "TRI $\mu$ P" and "Broken Mirros and Drifting Constants".